www.czasopisma.pan.pl PAN www.journals.pan.pl
Chemical and Process Engineering 2021, 42 (2), 91–104
DOI: 10.24425/cpe.2021.137343

Power characteristics of inline rotor-stators with different head designs

Alex Hannam[1], Trevor Sparks[2], N. Gül Özcan-Taşkın[1]

[1]Loughborough University, School of Chemical Engineering, Loughborough LE11 3TT, UK
[2]Independent Consultant

In-line rotor-stators are widely used for power intensive industrial applications, such as deagglomeration, emulsification. There is limited information on characteristic power numbers for different designs which can be used to calculate the average power input as a means to evaluate process performance. This study made use of 18 different rotor-stators, 17 of which were toothed designs with different geometry, and also a commercially available design, with the objectives of evaluating the applicability of different expressions for characteristic power numbers and establishing the effects of geometric variations on the power input.

The expression $P = Po_1\rho N^3D^5 + Po_2\rho N^2D^2Q$ is found to account for the experimental data over a wide range of operating conditions.

Rotor diameter was found to have the most prominent effect on the power input: an increase in rotor diameter from 119.6 to 123.34 mm resulted in an increase in the average power draw. The effect of rotor diameter examined with geometrically similar set ups reducing the diameter from 123.34 to 61.44 mm, for which the mixing chamber was also proportionately smaller, showed a decrease in the power input at a given speed and flowrate as well. The effects relating to the percentage of open area of the stator and number of rotor teeth were less obvious. Increasing the open area resulted in an increase in the power input – an effect which could be observed more clearly as the flowrate (1 to 4 l/s) and rotor speed (at 2000 and 3000 rpm) were also increased. Increasing the number of stator teeth increased the power input and this effect was more prominent when operating at the highest rotor speed of 3000 rpm and at low flowrates (1–2 l/s).

Keywords: in-line rotor-stators, power characteristics, rotor-stator design

1. INTRODUCTION

Rotor-stators are widely used for the manufacture of numerous products which require size reduction (deagglomeration, emulsification) or involve a fast chemical reaction. Vashisth et al. (2021) provide a good overview of these. The mixing head consists of a rotor operating at a high speed (typically thousands of rpm) in close proximity to a stator and other design features such as teeth, holes and/or blades contribute to the high levels of energy dissipation within the head which make these devices suitable for power intensive applications (Atiemo-Obeng and Calabrese, 2004). Whilst batch rotor-stators are more commonly used

* Corresponding author, e-mail: N.Ozcan-Taskin@lboro.ac.uk

during product development or formulation, in-line devices find applications in industrial scale manufacture allowing, typically, 100's of litres to be processed.

A knowledge of the average power input is essential for process design that targets size reduction to promote a reaction (for example van Kouwen et al., 2021; Meeuwse et al., 2010) or generate a fine dispersion (Atiemo-Obeng and Calabrese, 2004; Carillo de Hert et al., 2017; Håkansson et al., 2016; Özcan-Taşkin et al., 2009; Padron et al., 2001; Padron et al., 2008). Average power input from a batch rotor-stator, P, is obtained using the power number, Po, expression for tanks stirred with impellers:

$$Po = \frac{P}{\rho N^3 D^5} \tag{1}$$

Characteristic power number values for several batch rotor stators are available and have been used to evaluate process performance (for example Doucet et al., 2005; Kamaly et al., 2017; Padron, 2001 and Padron, 2005; Utomo et al., 2009).

With in-line rotor-stators that can be utilised in either a single pass or multiple passes through a recycle loop around a holding vessel, operating conditions, such as rotor speed and flow rate, as well as the specific design, affect the flow characteristics through the device, the power input and thus the process performance (Cooke et al., 2011; Özcan-Taşkın et al., 2011 and Özcan-Taşkın et al., 2016). Different expressions for characteristic power numbers have been used to estimate the power input over a range of operating conditions for design and scale up.

Sparks (1996) based the power draw on the kinetic energy of the fluid with the following equation:

$$Po = \frac{P}{\rho N^2 D^2 Q} \tag{2}$$

He pointed out that values obtained at low flow rates are not well represented with this expression (for the particular scale and conditions when $Q < 1$ l/s).

The expression proposed Baldyga (2007) to calculate the power draw includes Po_1 and Po_2 as characteristic power numbers:

$$P = Po_1 \rho N^3 D^5 + Po_2 \rho N^2 D^2 Q \tag{3}$$

The first term in Eq. (3) represents the pumping action of the rotor and the second represents the inlet flow rate. This expression has since been widely used to obtain characteristic power numbers of in-line rotor-stators and Table 1 lists Po_1 and Po_2 values for in-line rotor-stators of different head designs vary – some have teeth, others holes and some designs include rotating blades.

Schönstedt et al. (2015), who compared Eqs. (1) and (2), reported that Eq. (2) represented well their experimental data with Conti TDS 1, 2, 3 and 5 inline rotor-stators.

This study made use of 18 different rotor-stator heads, 17 of which were toothed designs with differences in their geometry and a commercially available one with also blades. The objectives have been to evaluate the applicability of different expressions for characteristic power numbers and establish the effects of geometric variations on power input, specifically the rotor diameter, percentage of open area on the stator and number of stator teeth.

Table 1. Example values for power numbers used in Eq. (3) from previous work

Rotor-Stator	Po_1	Po_2
Silverson GPDH-SQHS (Özcan-Taşkın et al., 2011)	0.13	9.10
Silverson EMSC (Özcan-Taşkın et al., 2011)	0.11	10.50
Ytron Z (Özcan-Taşkın et al., 2011)	0.18	10.60
Silverson 150/250 MS using fine holes (Cooke et al., 2011)	0.15	9.36
Silverson 150/250 MS using standard holes (Cooke et al., 2011)	0.23	7.95
Silverson 150/250 MS using no screen (Cooke et al., 2011)	0.22	7.16
Silverson 150/250 MS Mixer (Hall et al., 2011)	0.23	7.46
088/150 UHS mixer (Hall et al., 2011)	0.25	9.59

2. EXPERIMENTAL

2.1. Experimental rig

The experimental rig, schematically shown in Fig. 1, included two 2.5 m^3 capacity tanks. These allowed the dispersion leaving the rotor-stator to be returned to either Tank 1 or Tank 2, and hence offered the flexibility to operate in single pass or multiple passes through the rotor-stator.

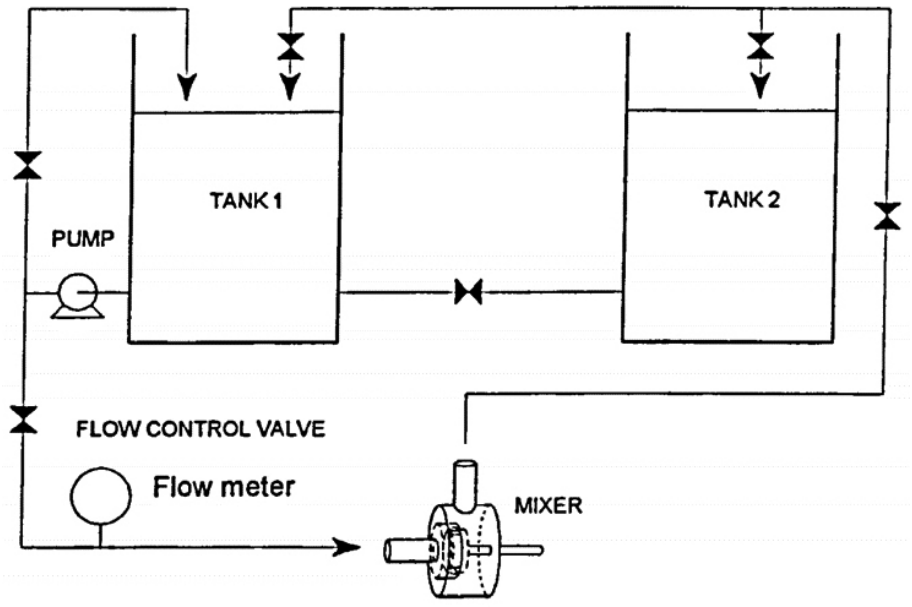

Fig. 1. Experimental rig

Water was pumped through the rig using a Flygt pump BS20066.171, connected to a frequency inverter thereby allowing pump speeds, hence flow rates to be controlled. A control valve was also used to adjust the liquid flow rate. The drive unit used, Silverson 425 LSM, was the same for all designs used.

2.2. Rotor-stator head geometries

A total of 18 rotor-stator head designs were studied. In all cases the rotor was held on the shaft by a bullet-shaped nut. Of these, 17 were in-house manufactured toothed designs to study the effects of geometric variations of the head. The "toothed" heads comprised trapezoidal teeth surrounding the circumference of the rotor and stator discs. These are representative of several commercially available designs. A schematic diagram along with a photograph are shown in Fig. 2a. The commercially available design, Silverson 425 LSM, used had rotor blades as shown in Fig. 2a.

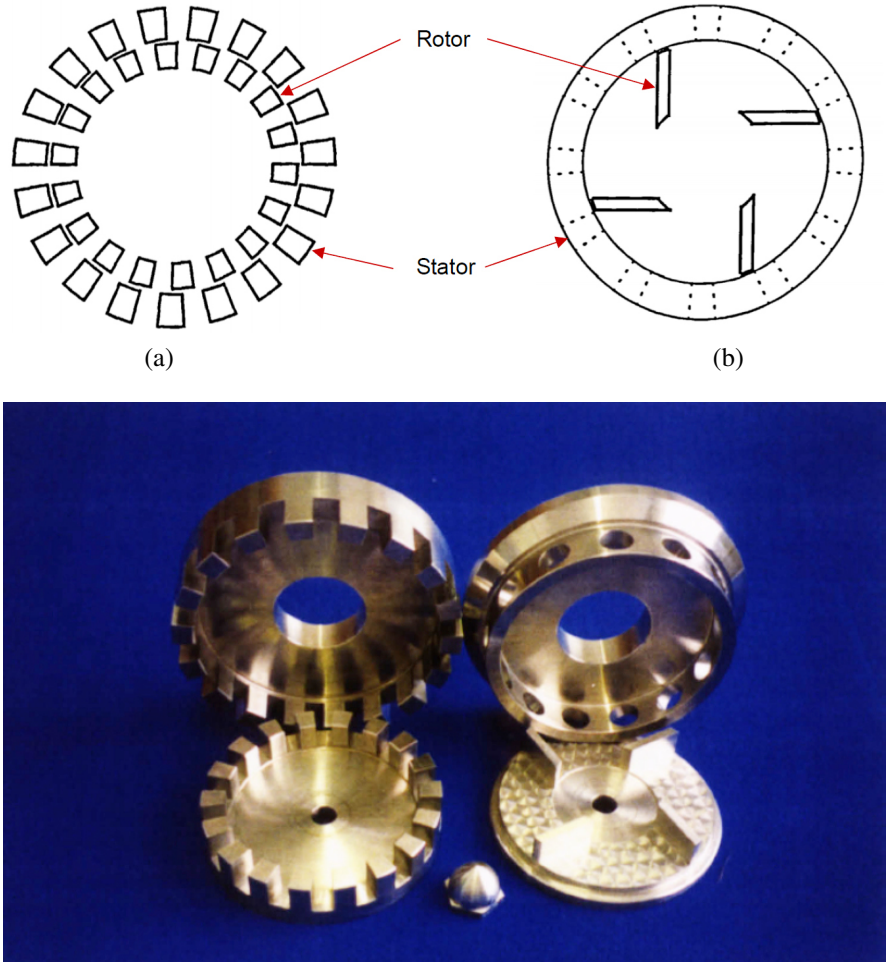

Fig. 2. Schematic drawing and photograph of a) toothed head and b) the Silverson 425 LSM head (rotation in clockwise direction)

All head designs used are listed in Table 2 which also contains a classification code for each toothed head to describe the rotor and stator combination. For example, $r/18/50/119.6$ describes a rotor, r, with 18 teeth, 50% open area and an outer diameter of 119.6 mm; and $s/19/50/123.8$ describes a stator, s, with 19 teeth, 50% open area and an inner diameter of 123.8 mm. For 16 of the 17 toothed heads used, 4 rotors and 4 stators were of different geometries to investigate the effect of geometric variables. One final toothed design, Case 17, with the classification code of $r/18/50/61.44$ and $s/18/50/61.9$, was fabricated at half-scale. Table 2 also includes values for gap between the rotor and stator. The Silverson head, which had the 0.23 mm gap width, as that of the half-scale head, had a rotor diameter of 107.95 mm.

The standard Silverson 425 LSM casing was used for all heads with the exception of the half scale toothed design, Case 17, for which a scaled casing was used.

Table 2. Rotor stator geometries studied

Case	Rotor-stator	Gap (mm)	Re ($ND^2\rho/\mu$)
1	*r*/18/50/119.6 & *s*/18/50/123.8	2.100	$1.4 \times 10^4 - 3.1 \times 10^6$
2	*r*/18/50/119.6 & *s*/18/33/123.8	2.100	$1.4 \times 10^4 - 3.1 \times 10^6$
3	*r*/18/50/119.6 & *s*/19/50/123.8	2.100	$1.4 \times 10^4 - 3.1 \times 10^6$
4	*r*/18/50/119.6 & *s*/36/50/123.8	2.100	$1.4 \times 10^4 - 3.1 \times 10^6$
5	*r*/12/67/121.45 & *s*/18/50/123.8	1.175	$1.6 \times 10^4 - 3.7 \times 10^6$
6	*r*/12/67/121.45 & *s*/18/33/123.8	1.175	$1.5 \times 10^4 - 3.6 \times 10^6$
7	*r*/12/67/121.45 & *s*/19/50/123.8	1.175	$1.5 \times 10^4 - 3.3 \times 10^6$
8	*r*/12/67/121.45 & *s*/36/50/123.8	1.175	$1.5 \times 10^4 - 3.3 \times 10^6$
9	*r*/18/50/121.45 & *s*/18/50/123.8	1.175	$1.5 \times 10^4 - 3.3 \times 10^6$
10	*r*/18/50/121.45 & *s*/18/33/123.8	1.175	$1.5 \times 10^4 - 3.3 \times 10^6$
11	*r*/18/50/121.45 & *s*/19/50/123.8	1.175	$1.5 \times 10^4 - 3.3 \times 10^6$
12	*r*/18/50/121.45 & *s*/36/50/123.8	1.175	$1.5 \times 10^4 - 3.3 \times 10^6$
13	*r*/18/50/123.34 & *s*/18/50/123.8	0.230	$1.6 \times 10^4 - 3.5 \times 10^6$
14	*r*/18/50/123.34 & *s*/18/33/123.8	0.230	$1.6 \times 10^4 - 3.5 \times 10^6$
15	*r*/18/50/123.34 & *s*/19/50/123.8	0.230	$1.7 \times 10^4 - 3.6 \times 10^6$
16	*r*/18/50/123.34 & *s*/36/50/123.8	0.230	$1.7 \times 10^4 - 3.6 \times 10^6$
17	*r*/18/50/61.44 & *s*/18/50/61.9	0.230	$5.1 \times 10^2 - 1.1 \times 10^5$
18	Silverson 425 LSM	0.230	$1.6 \times 10^4 - 3.7 \times 10^6$

2.3. Operating conditions

Water flow rates of up to 5 l/s were covered. The lowest flow rate was in most cases 0.5 l/s and in a few cases even lower flow rates were used. Rotor speeds ranged from 500 to 3000 rpm and corresponding rotor Reynolds numbers are also included in Table 2.

2.4. Measurement of flow rate

The liquid flowrate was measured using a magnetic flow meter, Altometer SC80 AS.

2.5. Determination of power input

The rotor shaft was split and a T 30 FD torque transducer, connected to a KMN 902.D signal amplifier, was fitted between flexible couplings to measure torque. Both were from Hottinger Baldwin Messtechnik.

Data analysis took into consideration losses determined as described by Sparks (1996) and only torque values higher than 1.5 times the losses were considered. This meant omitting only 1 to 3 values at the lowest speed of 500 rpm in a few cases and the resulting power numbers were not significantly different to those obtained including all data.

3. RESULTS AND DISCUSSION

3.1. Characteristic Power Numbers

Using the wide range of data available, different approaches, namely Eqs. (1), (2) and (3), were evaluated by comparing calculated power input values to those measured. Since the liquid flowrate is not considered in Eq. (1), results appear classified per rotor speed as shown in Figure 3a for Case 13 and Fig. 4a for Case 7. Therefore, this expression used for batch rotor-stators or stirred tanks (batch or continuous flow) is not suitable for estimating the power input with in-line rotor-stators.

Whilst calculated power values using Eq. (2) are in agreement with the experimental data at high liquid flow rates, Eq. (3) accounts for the data across the whole range. Example comparisons are shown in Fig. 3b and Fig. 3c for Case 13 and Fig. 4b and 4c for Case 7. The data set of Case 13 was obtained for flow rates greater than 0.5 l/s whereas data in Case 7 contains lower flow rates. Hence, Eq. (2) can be suitable if the flowrate range is sufficiently high but as Eq. (3) provides a good estimate of the power input by in-line rotor-stators across a wide range, it has been used to obtain characteristic power numbers for the different designs studied. Po_1 and Po_2 values obtained are shown in Table 3. Overall, these are of a similar order of magnitude to those reported with other rotor-stators in Table 1. Of these, the Ytron Z is also a toothed design with 3 rows of teeth in the rotor and stator.

Table 3. Rotor stator geometries studied

Case	Rotor-stator	Po_1	Po_2	Re
1	*r*/18/50/119.6 & *s*/18/50/123.8	0.075	8.72	$1.4 \times 10^4 - 3.1 \times 10^6$
2	*r*/18/50/119.6 & *s*/18/33/123.8	0.061	8.41	$1.4 \times 10^4 - 3.1 \times 10^6$
3	*r*/18/50/119.6 & *s*/19/50/123.8	0.085	8.45	$1.4 \times 10^4 - 3.1 \times 10^6$
4	*r*/18/50/119.6 & *s*/36/50/123.8	0.106	8.09	$1.4 \times 10^4 - 3.1 \times 10^6$
5	*r*/12/67/121.45 & *s*/18/50/123.8	0.071	8.19	$1.6 \times 10^4 - 3.7 \times 10^6$
6	*r*/12/67/121.45 & *s*/18/33/123.8	0.045	8.47	$1.5 \times 10^4 - 3.6 \times 10^6$
7	*r*/12/67/121.45 & *s*/19/50/123.8	0.082	8.54	$1.5 \times 10^4 - 3.3 \times 10^6$
8	*r*/12/67/121.45 & *s*/36/50/123.8	0.072	8.55	$1.5 \times 10^4 - 3.3 \times 10^6$
9	*r*/18/50/121.45 & *s*/18/50/123.8	0.063	8.99	$1.5 \times 10^4 - 3.3 \times 10^6$
10	*r*/18/50/121.45 & *s*/18/33/123.8	0.036	9.03	$1.5 \times 10^4 - 3.3 \times 10^6$
11	*r*/18/50/121.45 & *s*/19/50/123.8	0.055	9.08	$1.5 \times 10^4 - 3.3 \times 10^6$
12	*r*/18/50/121.45 & *s*/36/50/123.8	0.066	9.41	$1.5 \times 10^4 - 3.3 \times 10^6$
13	*r*/18/50/123.34 & *s*/18/50/123.8	0.041	10.57	$1.6 \times 10^4 - 3.5 \times 10^6$
14	*r*/18/50/123.34 & *s*/18/33/123.8	0.033	10.69	$1.6 \times 10^4 - 3.5 \times 10^6$
15	*r*/18/50/123.34 & *s*/19/50/123.8	0.034	10.70	$1.7 \times 10^4 - 3.6 \times 10^6$
16	*r*/18/50/123.34 & *s*/36/50/123.8	0.053	10.33	$1.7 \times 10^4 - 3.6 \times 10^6$
17	r/18/50/61.44 & s/18/50/61.9	0.201	8.38	$5.1 \times 10^2 - 1.1 \times 10^5$
		0.202	8.35	$1.4 \times 10^4 - 1.1 \times 10^5$
18	Silverson 425 LSM	0.050	6.21	$1.6 \times 10^4 - 3.7 \times 10^6$

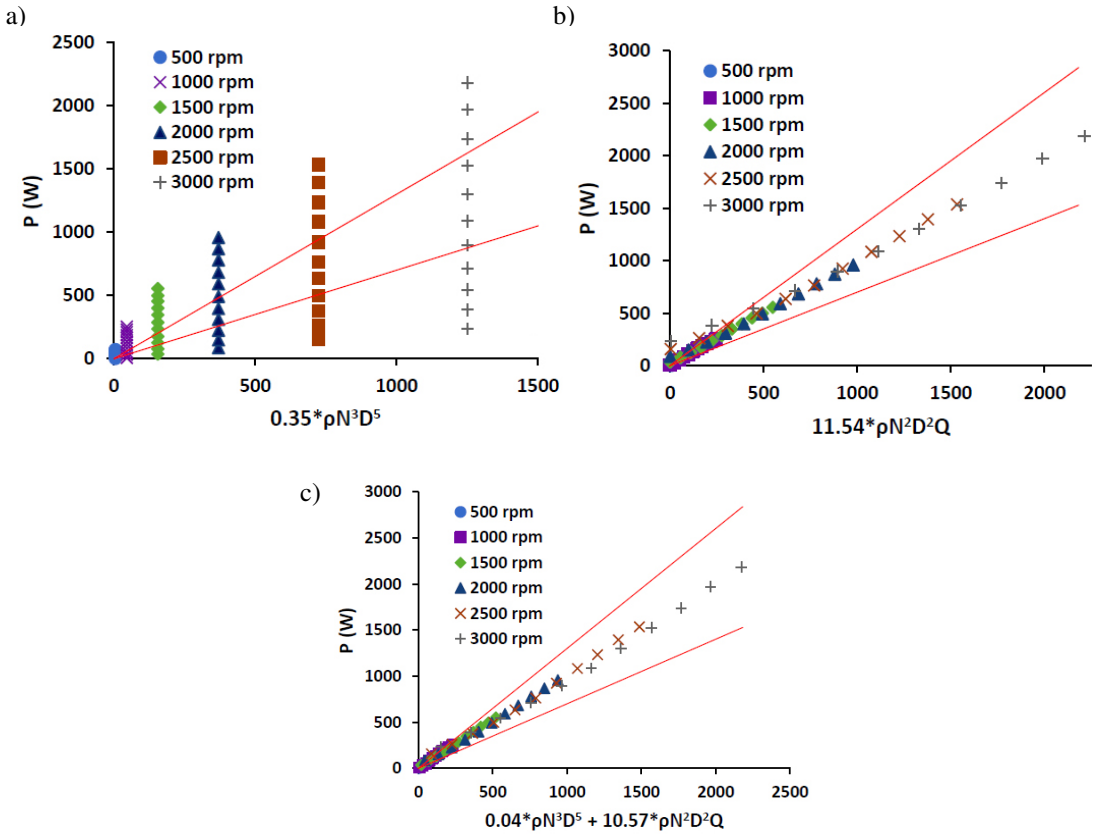

Fig. 3. Evaluation of different approaches to estimate the power draw for Case 13 (r/18/50/123.34 & s/18/50/123.8) using a) Eq. (1), b) Eq. (2) and c) Eq. (3)

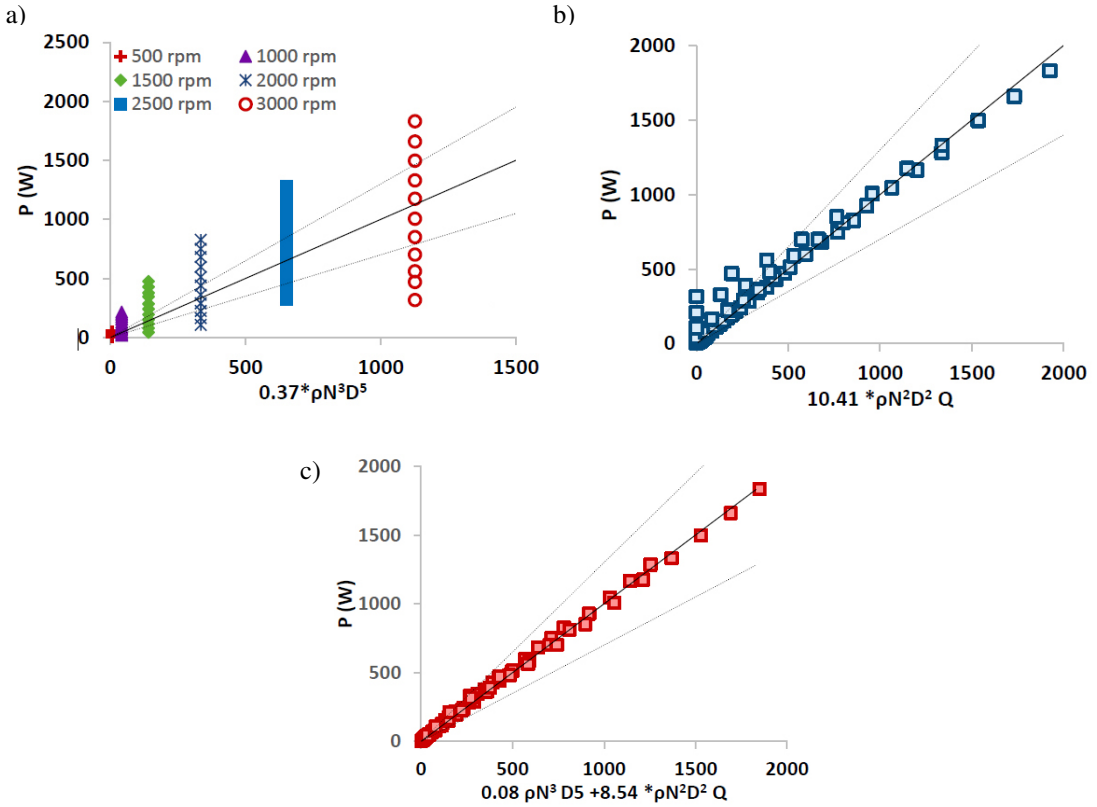

Fig. 4. Evaluation of different approaches to estimate the power draw for Case 13 (r/18/50/123.34 & s/18/50/123.8) using a) Eq. (1), b) Eq. (2) and c) Eq. (3)

It is worth pointing out that whilst Re > 10^4 in most cases, with the "half-toothed" design, i.e. Case 17, Reynolds number values were lower due to the smaller rotor diameter. Case 17 data for Re > 4×10^3 gave the same power number values as those for the whole data set and for Re > 1.4×10^4, there was a very slight change in Po_1 and Po_2 values (Table 3). It can therefore be concluded that the characteristic power number values remain constant at Reynolds numbers as low as about 500. Previous work (Padron and Özcan-Taşkın, 2018) with a different rotor-stator had shown this to be the case for Re > 10^3.

For the part of the study that related to the effect of geometric variations in the head design, Eq. (3) was considered.

3.2. Effect of rotor diameter on the characteristic Power Numbers

From Table 2, Cases 1, 5 and 13; Cases 2, 6 and 14; Cases 3, 7, and 15; and Cases 4, 8 and 16 were used to study the effect of rotor diameter on the characteristic power numbers and power input. For each cluster of Cases, stator geometry is given.

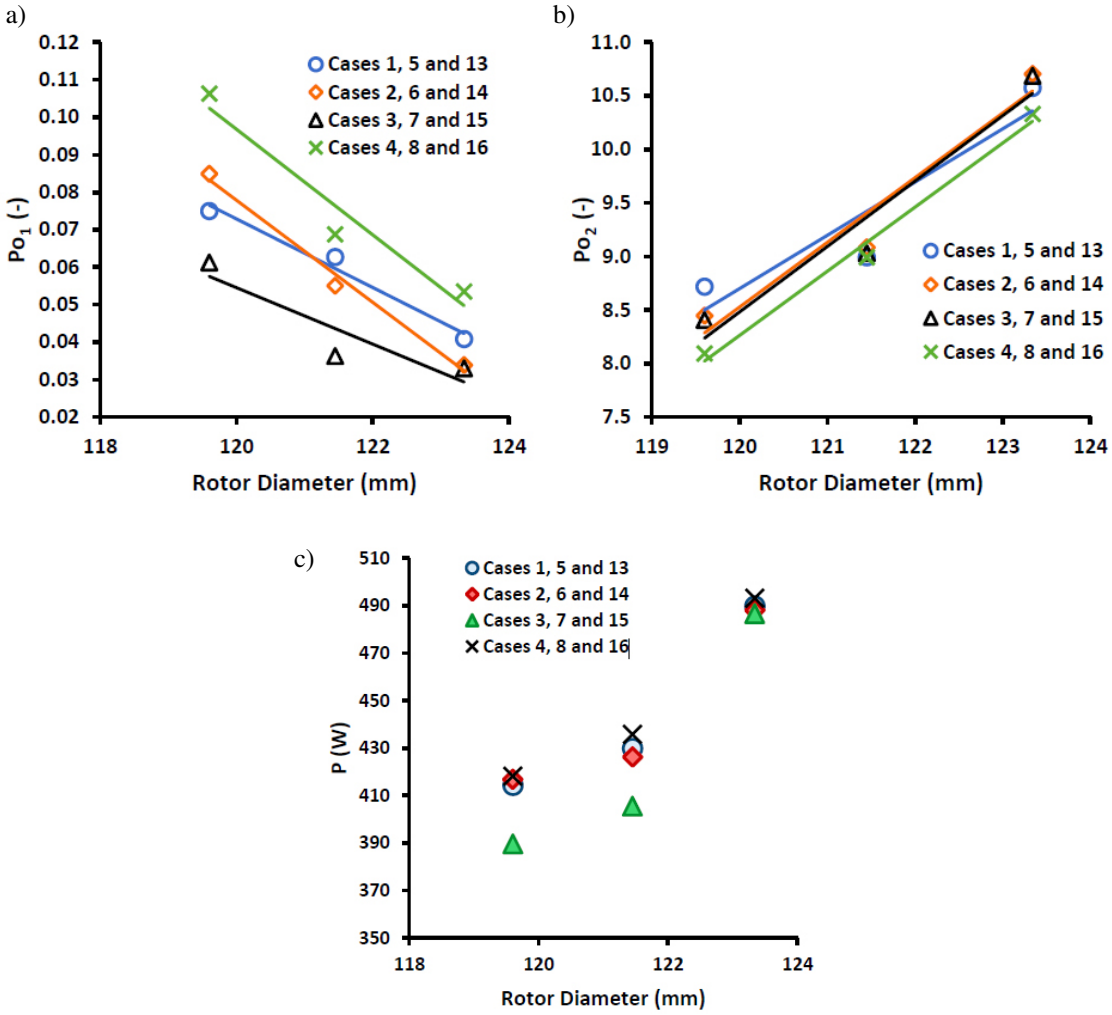

Fig. 5. Effect of rotor diameter on (a) Po_1, (b) Po_2, (c) average power input at 2000 rpm and 2.5 l/s

For all cases, the values of Po_1 decrease when the rotor diameter is increased (Fig. 5a). On the other hand, the values of Po_2 increase (Fig. 5b), which results in an increase in the overall power input (Fig. 5c). These results agree with those reported for batch rotor-stators which also show that an increase in rotor diameter is accompanied by an increase in power consumption (Yang et al., 2020).

For Cases 1, 5 and 13, the rotor speed and flowrate were varied to establish the combined effects of operating conditions and rotor diameter on the power draw as shown in Fig. 6.

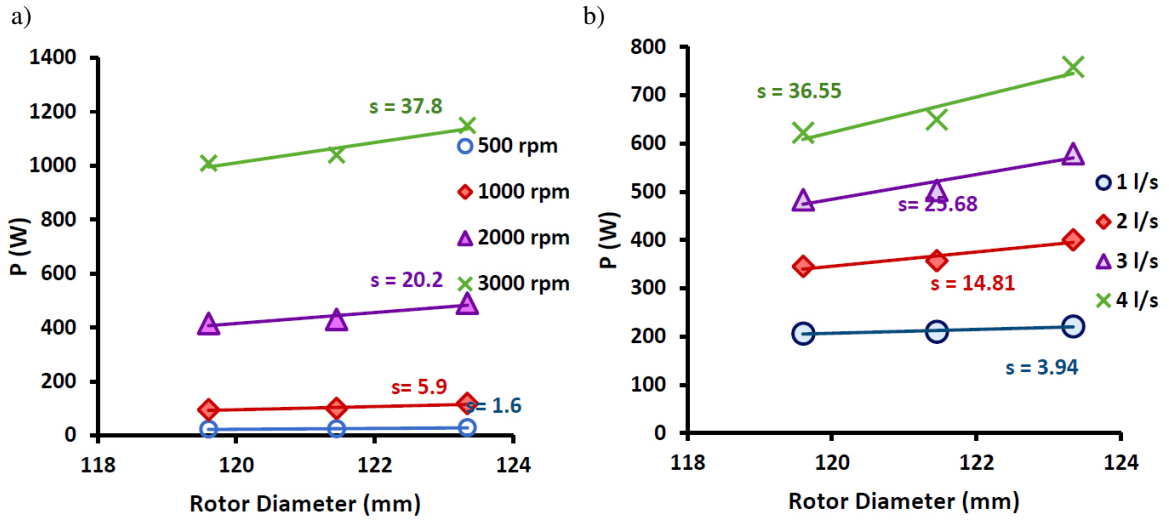

Fig. 6. Effect of rotor diameter on power input for Cases 1, 5 and 13 at (a) 2.5 l/s and (b) 2000 rpm

It can be seen in this Figure which includes the slopes, s, that the effect of rotor diameter on power input becomes more significant at high rotor speed and/or liquid flowrates.

These refer to variations in the rotor diameter within the range of 119.6 to 123.34 mm using a given mixing chamber. A comparison of the power input with Case 16 and Case 17 highlights the effect of doubling the rotor diameter, from 61.44 to 123.34 mm, due to change of scale. The smaller scale head has a considerably higher value of Po_1, and a smaller value of Po_2, further agreeing that a decrease in rotor diameter increases Po_1 and decreases Po_2. At a given rotor speed and flowrate, the power input by the smaller scale head (Case 17) is lower than its counter-part at larger scale (Case 16): at a speed of 3000 rpm and a flowrate of 3.2 l/s, power input values are 274 and 317 W, respectively.

3.3. Effect of the open area of the stator

From Table 2, Cases 1 and 2; Cases 5 and 6; Cases 9 and 10; and Cases 13 and 14 were considered to study the effect of the open area of the stator on the characteristic power numbers and power input. Increasing the open area of the stator increases the value of Po_1 (Fig. 7a), but the effect was negligible for Po_2 (Fig. 7b). This suggests that Po_2 value could be taken constant when the open area on the stator is varied. The effect on the average power input is minimal: a slight increase was noted with increasing open area (Fig. 7c). These findings are consistent with those for batch rotor-stators by Utomo et al. (2009) who reported that the power number increases as the total open area is increased. The head design in their study had holes instead of teeth.

For Cases 1 and 2, the combined effects of operating conditions and percentage of open area of the stator studied are shown in Figure 8. The effect became prominent at the highest speed of 3000 rpm; at lower rotor speeds, the power input is practically independent of the percentage of stator open area indicated by the low values of the gradient, s, (Fig. 8a). Similarly, the effect becomes more prominent as the liquid flow rate was increased (Fig. 8b).

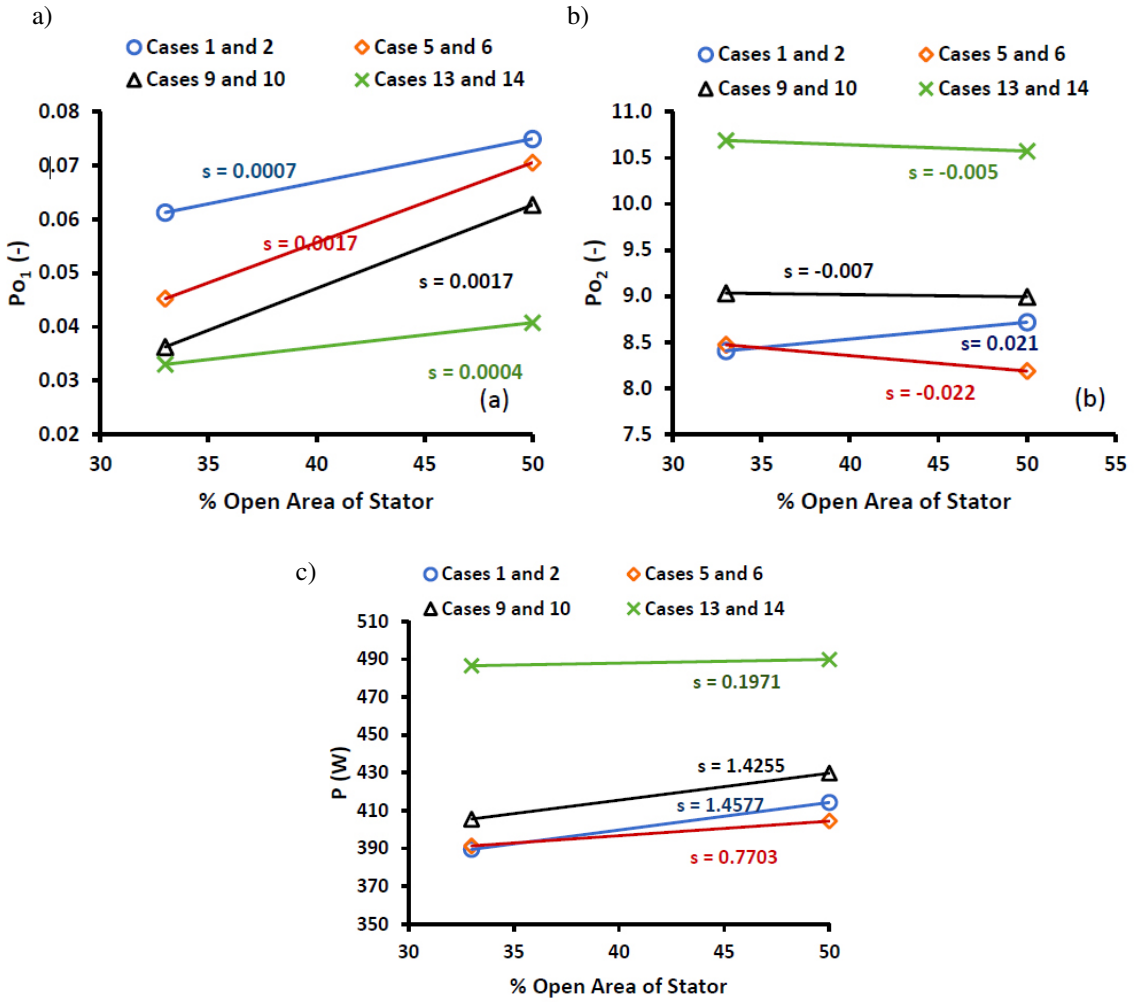

Fig. 7. Effect of percentage of open area of the stator compared to (a) Po_1, (b) Po_2 and (c) power input at 2000 rpm and 2.5 l/s

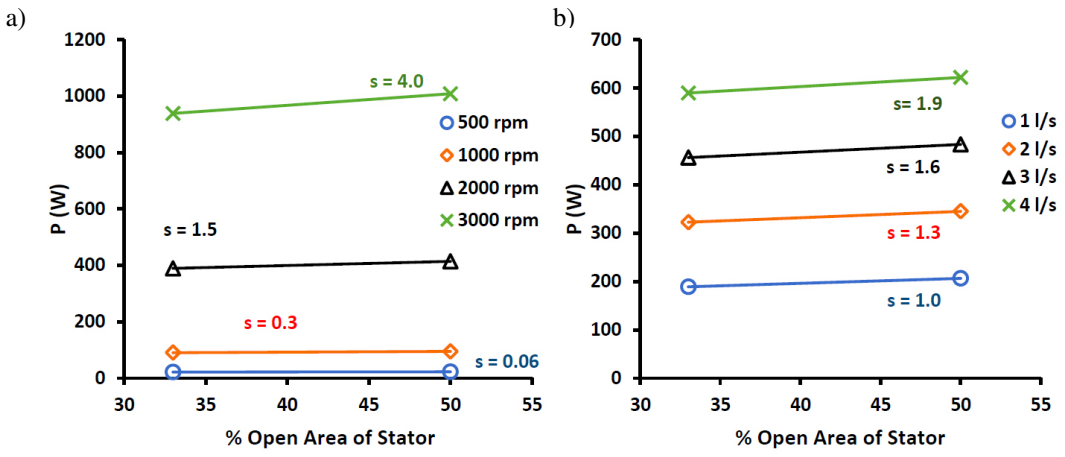

Fig. 8. Effect of percentage of open area of the stator on power input for Cases 1, 5 at a) 2.5 l/s and b) 2000 rpm

3.4. Effect of the number of stator teeth

From Table 2 Cases 1, 3 and 4; Cases 5, 7 and 8; Cases 9, 11 and 12; and Cases 13, 15 and 16 were used to study the effect of the open area of the stator on the characteristic power numbers and power input. It is worth pointing out that, for each cluster of Cases, the percentage of open area on both the rotor and stator is the same.

Overall, it appears that the value of Po_1 increases with an increase in the number of stator teeth (Fig. 9a). The percentage change in the values of Po_2 is small (Fig. 9b). When evaluated in terms of power input, the effect of number of teeth within the range studied seems negligible, as shown in Fig. 9c.

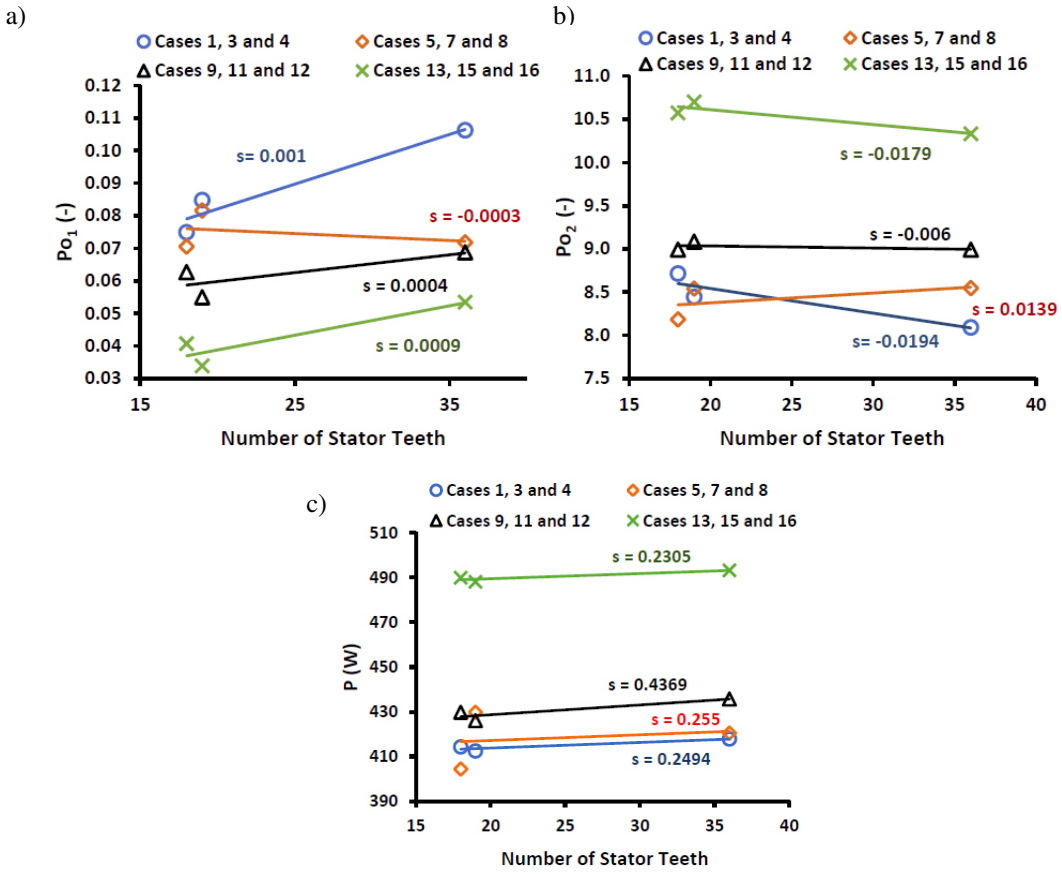

Fig. 9. The effect of varying the number of stator teeth on a) Po_1, b) Po_2 and (c) the power input at 2000 rpm and 2.5 l/s

For Cases 1, 3 and 4, the combined effects of operating conditions and number of stator teeth are studied. It appears that increasing the number of stator teeth slightly increases the average power input at the highest rotor speed and low flowrates in this study, i.e. 3000 rpm (Fig. 10a) and 1.0 and 2.0 l/s (Fig. 10b). A previous study that considered the effect of varying the number of holes maintaining the same open area

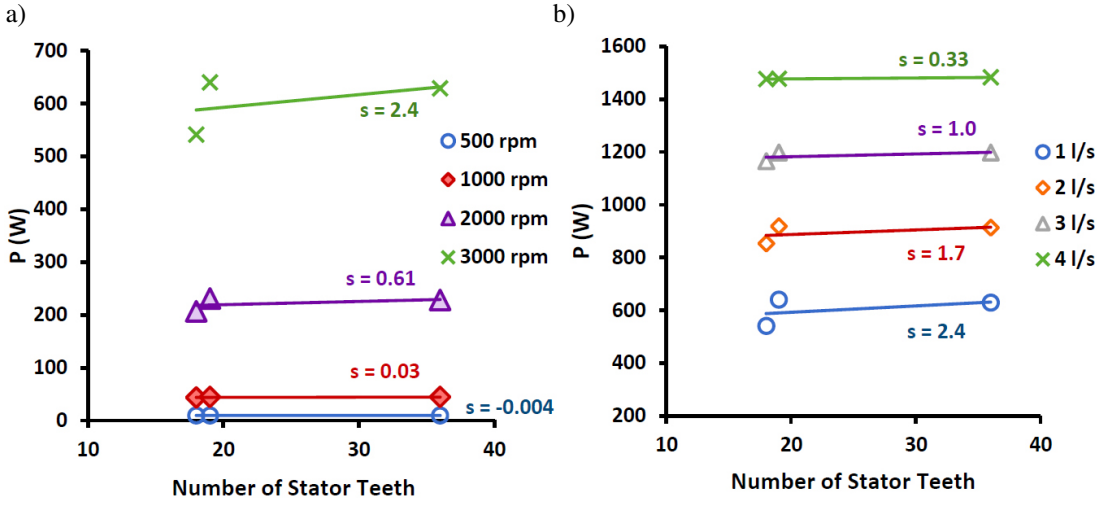

Fig. 10. Effect of the number of stator teeth on power for Cases 1, 2 and 3 at (a) 1 l/s and (b) 3000 rpm

has shown that for an inline rotor-stator with a varying number of holes, the power consumption increases and then decreases with the number of holes (Qin et al., 2017). It is difficult to make direct comparisons with those results as the variation was achieved by increasing the number of holes from 120 to 400.

4. CONCLUSIONS

Power input by 18 in-line rotor-stators was studied to obtain characteristic power numbers and determine the effects of geometric variations of the head design. Of these, 17 were toothed heads and one commercial design also had blades on the rotor.

An evaluation of different approaches to determine power numbers characteristic of a design has shown that the power number defined for batch systems (Eq. (1)) is not suitable for in-line rotor-stators. Whilst Eq. (2) gives an estimate compared to experimentally measured values at sufficiently high flowrates ($Q > 1$ l/s for this scale), the following expression, i.e. Eq. (3), represents data over a wide range of conditions, particularly in terms of liquid flowrate.

Reynolds numbers were higher than 1.5×10^4 in practically all cases, with the exception of one for which $\mathrm{Re} > 502$. Analysis of data for this case considering $\mathrm{Re} > 10^3$ or $\mathrm{Re} > 10^4$ did not show a significant difference in the power number values obtained compared to those with data included, suggesting that for in-line rotor-stators power numbers can be taken to be constant for $\mathrm{Re} > 500$. Whilst power numbers are readily available for different impeller types and many batch rotor-stator designs, the information is limited for inline rotor-stator designs. Hence, the values reported from this study can be useful for calculating the power input with the specific designs or approximate values for similar designs.

The study also aimed at establishing how geometric variations on the rotor-stator head, namely the rotor diameter, percentage of open area of stator and number of teeth, may affect the power input. Of these, the effect of rotor diameter appears to be the most prominent: an increase in rotor diameter (119.6 to 123.34 mm), and hence a decrease in the gap between the rotor and stator, decreases Po_1 and increases Po_2, resulting in an overall increase in the power draw for any rotor speed and flowrate. The effect of rotor diameter was also studied within the context of scale up of the head and when the diameter was reduced from 123.34 to 61.44 mm using a proportionately smaller mixing chamber, the power input decreased (for example at 3000 rpm and 3.2 l/s, the power input was 274 and 317 W with the small and large units respectively).

Increasing the percentage of open area of stator resulted in an increase in the power input- an effect which became more obvious as the flow rate was increased from 1 to 4 l/s and primarily at high speeds (2000 and 3000 rpm).

Increasing the number of stator teeth increased the power input at the highest rotor speed of 3000 rpm and at low flowrates (1–2 l/s).

These findings would be useful for the design of rotor-stator heads as well as process design and scale up to match the requirements of the product and process with the power input. Further work can make use of more viscous and non-Newtonian liquids.

SYMBOLS

D rotor diameter, m
N rotor speed, s^{-1}

P power, W
Po power number, (–)
Q flowrate, m^3/s
Re Reynolds number, (–)

Greek symbols

ρ liquid density, kg/m^3
μ viscosity, Pa·s

ACKNOWLEDGMENTS

Trevor Sparks would like to acknowledge the support from the industrial members of the HILINE (High Intensity In-Line Mixing) Consortium as well as colleagues at BHR Group Ltd, and in particular John Brown.

REFERENCES

Atiemo-Obeng V.A., Calabrese R.V., 2004. Rotor–stator mixing devices, In: Paul E.L., Atiemo-Obeng V.A., Kresta,S.M. (Eds.), *Handbook of industrial mixing*. John Wiley & Sons, Inc., Hoboken, NJ, USA, 479–505. DOI: 10.1002/0471451452.ch8.

Baldyga J., Kowalski A.J., Cooke M., Jasinska M., 2007. Investigation of micromixing in a rotor-stator mixer. *Chem. Process Eng.*, 28 (4), 867-877.

Carrillo De Hert S., Rodgers T.L., 2017. Continuous, recycle and batch emulsification kinetics using a high-shear mixer. *Chem. Eng. Sci.*, 167, 265–277. DOI: 10.1016/j.ces.2017.04.020.

Cooke M., Rodgers T.L., Kowalski A.J., 2011. Power consumption characteristics of an in-line silverson high shear mixer. *AIChE J*., 58, 1683-1692. DOI: 10.1002/aic.12703.

Doucet L., Ascanio G., Tanguy P.A., 2005. Hydrodynamics characterisation of rotor-stator mixer with viscous fluids. *Chem. Eng. Res. Des.*, 83, 1186-1195. DOI: 10.1205/cherd.04254.

Håkansson, A., Chaudhry, Z., Innings, F., 2016. Model emulsions to study the mechanism of industrial mayonnaise emulsification. *Food Bioprod. Process.*, 98, 189–195. DOI: 10.1016/j.fbp.2016.01.011.

Hall S., Cooke M., Pacek A.W., Kowalski A J., Rothman D., 2011. Scaling up of silverson rotor–stator mixers. *Can. J. Chem. Eng.*, 89, 1040-1050. DOI: 10.1002/cjce.20556.

Kamaly S.W., Tarleton A.C., Özcan-Taşkın N.G., 2017. Dispersion of clusters of nanoscale silica particles using batch rotor-stators. *Adv. Powder Technol.*, 28, 2357-2365. DOI: 10.1016/j.apt.2017.06.017.

Meeuwse M., van der Schaaf J., Kuster B. F. M., Schouten,J. C., 2010. Gas–liquid mass transfer in a rotor–stator spinning disc reactor. *Chem. Eng. Sci.*, 65, 466-471. DOI: 10.1016/j.ces.2009.06.006.

Özcan-Taşkın G., Kubicki D., Padron G., 2011. Power and flow characteristics of three rotor-stator heads. *Can. J. Chem. Eng.*, 89, 1005-1017. DOI: 10.1002/cjce.20553.

Özcan-Taşkin G., Padron G., Voelkel A., 2009. Effect of particle type on the mechanisms of break up of nanoscale particle clusters. *Chem. Eng. Res. Des.*, 87, 468-473. DOI: 10.1016/j.cherd.2008.12.012.

Özcan-Taşkin N.G., Padron G.A., Kubicki D., 2016. Comparative performance of in-line rotor-stators for deagglomeration processes. *Chem. Eng. Sci.*, 156, 186–196. DOI: 10.1016/j.ces.2016.09.023.

Padron G.A., 2005. *Effect of surfactants on drop size distribution in a batch, rotor-stator mixer*. PhD Thesis, University of Maryland.

Padron G.A., Eagles W.P., Őzcan-Taşkin G.N., McLeod G., Xie L., 2008. Effect of particle properties on the breakup of nanoparticle clusters using an in-line rotor-stator. *J. Dispersion Sci. Technol.*, 29, 4, 580-586. DOI: 10.1080/01932690701729237.

Padron G., 2001. *Measurement and comparison of power draw in batch rotor-stator mixers*. MSc Thesis, Department of Chemical Engineering, University of Maryland.

Padron G.A., Özcan-Taşkın N.G., 2018. Particle de-agglomeration with an in-line rotor-stator mixer at different solids loadings and viscosities. *Chem. Eng. Res. Des.*, 32, 913-921. DOI: 10.1016/j.cherd.2018.01.041.

Qin H., Xu Q., Li W., Dang,X., Han Y., Lei K., Zhou L., Zhang J., 2017. Effect of stator geometry on the emulsification and extraction in the inline single-row blade-screen high shear mixer. *Ind. Eng. Chem. Res.*, 56, 9376-9388. DOI: 10.1021/acs.iecr.7b01362.

Schönstedt B., Jacob H., Schilde C., Kwade A., 2015. Scale-up of the power draw of inline-rotor–stator mixers with high throughput. *Chem. Eng. Res. Des.*, 93, 12-20. DOI: 10.1016/j.cherd.2014.04.004.

Sparks T., 1996. *Fluid mixing in rotor–stators*. PhD Thesis, Cranfield University, Cranfield, UK.

Utomo A., Baker M., Pacek A., 2009. The effect of stator geometry on the flow pattern and energy dissipation rate in a rotor–stator mixer. *Chem. Eng. Res. Des.*, 87, 533–542. DOI: 10.1016/j.cherd.2008.12.011.

van Kouwen E.R., Winkenwerder W., Brentzel Z., Joyce B., Pagano T., Jovic S., Bargeman G., and van der Schaaf J., 2021. The mixing sensitivity of toluene and ethylbenzene sulfonation using fuming sulfuric acid studied in a rotor-stator spinning disc reactor. *Chem. Eng. Process.*, 160, 108303. DOI: 10.1016/j.cep.2021.108303.

Vashisth V., Nigam K.D.P., Kumar V., 2021. Design and development of high shear mixers: Fundamentals, applications and recent progress. *Chem. Eng. Sci.*, 232, 116296. DOI: 10.1016/j.ces.2020.116296.

Yang L., Li W., Guo J., Li W., Wang B., Zhang M., Zhang J., 2020. Effects of rotor and stator geometry on dissolution process and power consumption in jet-flow high shear mixers. Front. *Chem. Sci. Eng.*, 15, 384–398. DOI: 10.1007/s11705-020-1928-7.

Received 1 July 2021
Received in revised form 30 July 2021
Accepted 2 August 2021